J. Biochem. **138**, 687–695 (2005)
doi:10.1093/jb/mvi163

Nitration of Profilin Effects Its Interaction with Poly (L-Proline) and Actin

S. Kasina[1], Wasia Rizwani[2], K. V. N. Radhika[2] and Surya S. Singh[2,*]

[1]Hansen's Life Sciences Research Building, Department of Biological Sciences, Purdue University, West Lafayette, Indiana 47906, USA; and [2]Department of Biochemistry, University College of Science, Osmania University, Hyderabad-500 007, India

Received June 4, 2005; accepted August 27, 2005

Profilin from bovine spleen was nitrated with peroxynitrite; immunoblotting and spectrophotometric quantitation of nitrotyrosine residues suggested nitration of a single tyrosine residue in profilin with a stoichiometry of 0.6 mol of nitrotyrosine/mole of profilin. A decrease in the nitrotyrosine immunoreactivity of nitroprofilin during digestion with carboxypeptidase Y indicated that nitrotyrosine is located at the C-terminus of profilin. Nitroprofilin interaction with ligands such as phosphatidylinositol 4,5-bisphosphate, actin and poly (L-proline) was analyzed by monitoring the tryptophan fluorescence. Scatchard plot and binding isotherm data obtained revealed no significant difference in affinity of nitroprofilin to phosphatidylinositol 4,5-bisphosphate (K_d of 4.8 ± 0.5 μM for profilin, and K_d of 5.7 ± 0.6 μM for nitroprofilin), while poly (L-proline) binding studies revealed a twenty-fold increase in the affinity of profilin to poly (L-proline) upon nitration (K_d of 21.8 ± 1.7 μM for profilin, and K_d of 1.1 ± 0.1 μM for nitroprofilin). Actin polymerization studies involving pyrene-labeled actin indicated that profilin nitration inhibits the actin sequestering property of profilin. The critical actin monomer concentration (C_c) was 150 and 250 nM in the presence of nitroprofilin and profilin, respectively. Thus, nitric oxide and free radicals produced under different conditions could alter the functions of profilin through nitration, such as its interaction with actin and poly (L-proline).

Key words: actin, profilin, poly (L-proline), phosphatidylinositol 4, 5 bisphosphate, tyrosine nitration.

Abbreviations: LDL, low density lipoprotein; MOE, molecular operating environment; NT, nitrotyrosine; PI (4,5)-P2, PIP2, phosphatidylinositol 4,5-bisphosphate; PLP, poly (L-proline); VASP, vasodilator-stimulated phosphoprotein.

The peroxynitrite anion ($ONOO^-$), a product of the rapid reaction of nitric oxide with superoxide, is a potent and versatile endogenous reactant (*1*) that can attack a wide range of biological molecules, including lipids (*2*), DNA (*3*), and proteins (*4*), as well as smaller molecules such as ascorbate and glutathione (*5*). A major reaction of $ONOO^-$ with proteins results in the formation of NT. Tyrosine nitration is commonly and widely studied, and has been shown in a number of instances to affect protein function (*6–11*).

Peroxynitrite production has been observed in many inflammatory conditions, and current evidence suggests that $ONOO^-$ is a more potent and cytotoxic mediator than superoxide or nitric oxide alone (*12*). Recently, it was reported that profilin acts downstream of LDL to mediate diabetic endothelial cell dysfunction and an elevated level of profilin expression has been observed in atherosclerotic plaques (*13*). Abnormal platelet aggregation increases atherosclerosis and further narrows the internal diameter of arteries. Although there is substantial evidence for peroxynitrite-mediated nitrotyrosine (NT) formation in the pathophysiology of atherosclerosis (*14*, *15*), the effect of NT formation on profilin's function and its role in the pathogenesis of this disease remain virtually unknown. In an isolated study by Sabetkar *et al.* (*16*) on platelets, a number of cytoskeletal actin-binding proteins including profilin underwent nitration. A physiological site where profilin can meet peroxynitrite can be found in all inflammatory conditions.

Profilin is a ubiquitous, 12–15 kDa cytoskeletal protein that interacts specifically with actin, phosphoinositides and poly (L-proline). It links signaling pathways to actin cytoskeleton organization by binding to phosphoinositides and PLP stretches present in several proteins involved in signal transduction (*17–20*). Tyrosine nitration could be accompanied by changes in profilin's physicochemical properties and biological functions since fluorescence, site-directed mutagenesis, qualitative NMR and other studies indicated that tyrosine residues in profilin [6 (helix 1, N-terminal), 26 (β-strand), 128 (helix 4), and 139 (turn, C-terminal)] are important for binding to PLP, PI (4,5)-P_2 and actin (*21–26*). The bulky nitro group induces steric perturbations in the structure of tyrosine, which disrupts protein-protein interactions involving tyrosine residues. Whether profilin undergoes nitration upon peroxynitrite production and whether nitration of profilin has any effect on its ligand binding or interacting property have been investigated. Hence the present paper deals with the

*To whom correspondence should be addressed. Tel: +91-040-27097044, Fax: +91-040-27097044, E-mail: satyasingh123@rediffmail.com

in vitro nitration of profilin by peroxynitrite, and the influence of this modification on profilin's interactions with actin, PI (4,5)-P_2 and PLP.

MATERIALS AND METHODS

Cyanogen bromide–activated cross-linked 4% beaded agarose (CNBr-agarose CL4B) was obtained from Pharmacia. Tris [hydroxymethyl] aminomethane (Tris), urea, β-mercaptoethanol, poly-L-proline (8,000 Da), glycine, Triton X-100, Tween-20, adenosine triphosphate (ATP), gelatin, NBT/BCIP, anti–nitro tyrosine antibodies, carboxypeptidase Y and PMSF were from Sigma Chemical Co., St. Louis, USA. *N*-(1-pyrenyl) iodoacetamide was from Molecular Probes, Eugene, USA. PIP_2 was prepared from baker's yeast. Disposable spectrofluorimeter cuvettes were obtained from Bio-Rad. All other chemicals were locally purchased and were of analytical grade.

Software—Swiss-pdbviewer, MOE and Gromacs.

Buffers—Transfer buffer: 25 mM Tris, 192 mM glycine and 20% methanol. TTBS buffer: 10 mM Tris, 154 mM NaCl and 0.1%Tween-20, pH 7.5. Potassium phosphate buffer: 100 mM, pH 7.4, with 25 mM NH_4HCO_3 and 1 mM DTPA. Citrate buffer: 100 mM, pH 6.0, with trisodium citrate and citric acid. Fluorescence buffer: 10 mM Tris buffer, pH 7.6 containing 150 mM KCl, 1 mM EDTA, and 5 mM β-mercaptoethanol. Myosin extraction buffer: 0.5 M KCl and 0.1M K_2HPO_4. Buffer A: 2 mM Tris-HCl, pH 8.0, containing 0.2 mM ATP and 0.2 mM $CaCl_2$. G-buffer: 2 mM Tris-HCl, pH 7.2, containing 0.2 mM Ca^{2+}, 2 mM ATP, 0.2 mM DTT and 0.02% sodium azide. F-buffer: G-buffer containing 150 mM KCl and 2 mM Mg^{2+}.

Purification of Profilin—Profilin was purified from bovine spleen according to the procedure of Bhargavi and Singh (*27*). Protein concentrations were determined by the Lowry method (*28*), and the homogeneity was confirmed by electrophoresis on 10% SDS-polyacrylamide (Tricine) gels (*29*).

Synthesis of Peroxynitrite—Peroxynitrite was synthesized as previously described by Beckman *et al.* (*30*). Briefly, an aqueous solution of 0.6 M $NaNO_2$ was rapidly mixed with an equal volume of 0.7 M H_2O_2 containing 0.6 M HCl, and then immediately quenched with the same volume of 1.5 M NaOH. Excess H_2O_2 was removed by the addition of solid MnO_2. The mixture was shaken for 10 min at 4°C and then filtered to remove MnO_2. The filtrate was frozen at –20°C for 5–7 days. Peroxynitrite forms a yellow top layer around ice crystals due to freeze fractionation. The top layer typically contained 50–150 mM peroxynitrite, as determined from the UV-absorbance at 302 nm (*31*). Controls were prepared by the same procedure except that the addition of 1.5 M NaOH was delayed, leading to immediate decomposition of the oxidant formed. Working dilutions of both active and decomposed peroxynitrite were prepared in 0.1 M NaOH.

Profilin Nitration under In Vitro Conditions—Profilin (25 μM) in 100 mM potassium phosphate buffer, pH 7.4, was incubated with increasing concentrations of peroxynitrite (25, 50, 200, 400 and 600 μM) at room temperature for 30 min. Reaction was stopped by adding 4× SDS sample buffer, proteins were separated by 10% SDS-PAGE (*29*) and then transferred onto nitrocellulose membrane, and nitration was detected using anti-nitrotyrosine antibodies.

Spectrophotometric Quantitation of Profilin Nitration—Profilin (25 μM) in 100 mM potassium phosphate buffer, pH 7.4, was incubated with increasing concentrations of peroxynitrite (25, 50, 100, 250, 2,500, 5,000 and 10,000 μM) at room temperature for 30 min, and the reaction was quenched by placing the mixture on ice. The amount of nitrotyrosine formed upon peroxynitrite treatment was determined spectrophotometrically by measuring the specific absorbance at 428 nm ($\varepsilon = 4{,}200\ M^{-1}\ cm^{-1}$). Any background absorbance due to added peroxynitrite was subtracted. Control experiments were performed with decomposed peroxynitrite or the reverse order addition of peroxynitrite. The stoichiometry of profilin nitration was determined by calculating the moles of nitrotyrosine/mole profilin.

Carboxypeptidase Y Digestion of Nitroprofilin—Ten micrograms (1,000 mU) of carboxypeptidase Y was added to 150 μg of nitrated profilin, in 0.1 M sodium citrate buffer, pH 6.0, followed by incubation for 6, 12, 24 or 48 hours at 25°C. Digestion was stopped by adding phenylmethylsulfonyl fluoride (PMSF) to a final concentration of 5 mM. Loss of nitrotyrosine immunoreactivity was evaluated by probing Western blots with anti-nitrotyrosine antibodies.

Poly (L-Proline) and PI (4,5)-P_2–Binding Studies—The binding of PIP_2/PLP to profilin (10 μM) and nitroprofilin (10 μM) was monitored as the changes in tryptophan fluorescence using a Jasco FP750 spectrofluorimeter (*34*). The excitation wavelength was set to 295 nm, and emission spectra from 320 to 400 nm were recorded. The titration of profilin/nitroprofilin (10 μM) with PIP_2 and PLP was carried out by the addition of small aliquots of PIP_2 (2.25, 4.5, 9, 13.5, 18, 27, 36, 45, 63, 81 and 99 μM) and PLP (1, 1.5, 2, 3, 5, 10, 15, 20, 25, 30, 35, 40, 45 and 50 μM), respectively, at 20°C. Titrations were performed against appropriate blanks. The equilibrium dissociation constant/binding constant (K_d) of profilin and nitroprofilin binding to PIP_2 and PLP were calculated with a modified Scatchard equation where K_d is inversely proportional to affinity. Free ligand is assumed to be the amount of ligand added, since the amount of ligand bound to the protein is negligible (approximately 5–10 fold excess ligand) compared to the total ligand added.

Fluorescent Labeling of Actin—F-actin purified from rabbit skeletal muscle acetone powder was covalently labeled with the fluorescent dye *N*-(1-pyrenyl) iodoacetamide as described by Kouyama and Mihashi (*35*). The concentration of G-actin was determined by Folin-Lowry's method (*28*). The extent of labeling was calculated by using the molar absorption coefficient of the labeled actin monomer ($2.2 \times 10^4\ M^{-1}\ cm^{-1}$ at 344 nm).

Actin Polymerization Studies—Actin polymerization was studied by incubating 2 μM G-actin (10% pyrene-labeled) in F-buffer with 2 μM profilin or nitroprofilin and then the fluorescence intensity was measured at zero time and after 30 minutes incubation (excitation at 365 nm and emission at 407 nm) (*35*). The critical actin monomer concentration (C_c) for actin alone or actin in the presence of constant amounts of profilin or nitroprofilin was determined by measuring the decrease in the fluorescence of serially diluted samples of F-actin (supplemented with 10% of pyrene-labeled actin) after a preincubation period of 16 h at room temperature. The excitation and

emission wavelengths were set at 365 nm and 407 nm, respectively (*34–36*).

RESULTS

Profilin Nitration under In Vitro Conditions—Western blots of nitroprofilin probed with anti-nitrotyrosine antibodies showed a peroxynitrite concentration–dependent increase in the nitrotyrosine level (Fig. 1a). Spectrophotometric quantitation of nitrotyrosine in peroxynitrite-treated profilin indicated a stoichiometry of 0.6 (moles of nitrotyrosine/mole of profilin) with a 100-fold molar excess of peroxynitrite over profilin (Fig. 1b), indicating that a single tyrosine residue is nitrated in profilin.

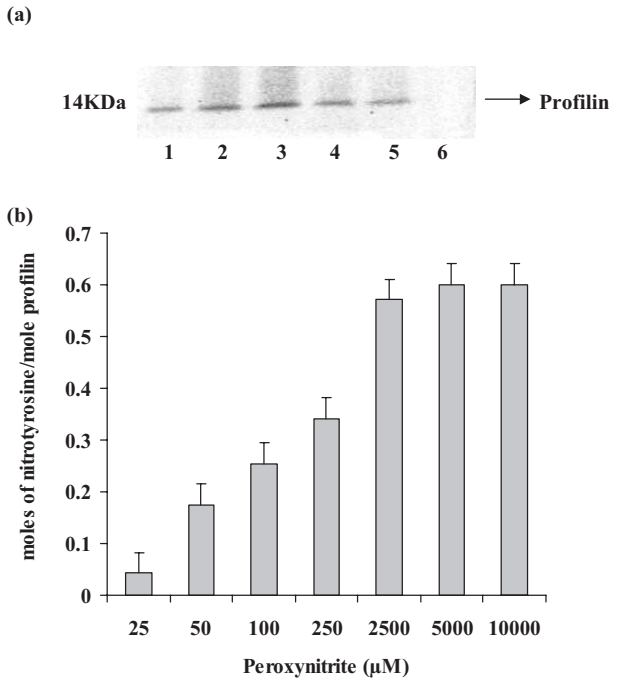

Fig. 1. ***In vitro* nitration of profilin.** (a) Immunodetection of nitrotyrosine residues. Profilin (25 μM) in 100 mM potassium phosphate buffer, pH 7.4, was treated with different concentrations of peroxynitrite (25, 50, 200, 400 and 600 μM) for 30 min at room temperature. Proteins were resolved by 10% SDS-PAGE, transferred to a nitrocellulose membrane and then immunoblotted with polyclonal anti-nitro tyrosine antibodies. Lane 1, 200 μM treated; lane 2, 400 μM treated; lane 3, 600 μM treated; lane 4, 100 μM; lane 5, 50 μM; lane 6, Control. (b) Stoichiometry of profilin nitration. Profilin (25 μM) in 100 mM potassium phosphate buffer, pH 7.4, was treated with different concentrations of peroxynitrite for 30 min. The amount of nitrotyrosine formed was determined spectrophotometrically by measuring the absorbance at 428 nm (ε = 4,200 M^{-1} cm^{-1}). The results are expressed as moles of nitrotyrosine/mole profilin and represent the means ± SEM of 4 independent experiments.

Carboxypeptidase Y Digestion of Nitroprofilin—Western blot analysis with anti-nitrotyrosine antibodies after digestion with carboxypeptidase for different times revealed a rapid decrease in the nitrotyrosine immunoreactivity of profilin (Fig. 2). Subsequently, immunoblotting with anti-profilin antibodies revealed no change in protein mass or additional bands of smaller molecular mass (Fig. 2). These results suggest that nitrotyrosine is located at the C-terminus of profilin.

Binding of Profilin/Nitroprofilin to PI (4,5)-P_2—Nitroprofilin exhibited a greater change in fluorescence (ΔF) against PIP_2 when compared to profilin (Fig. 3a). Both profilin and nitroprofilin exhibited saturation as to ΔF at higher PIP_2 concentration. The relative affinities of profilin and nitroprofilin to PIP_2 were determined through binding isotherms by plotting $\Delta F/\Delta F_{max}$ against PIP_2 concentration. The binding isotherms revealed that at different concentrations of PIP_2 the amount of PIP_2 bound is the same for profilin and nitroprofilin, indicating similar affinities (Fig. 3b). Further, the binding constant (K_d) was calculated from Scatchard plots, where $\Delta F/\Delta F_{max}$ was plotted against $\Delta F/\Delta F_{max}$/Lfree. Figure 3c indicates a K_d of 4.8 ± 0.5 μM for profilin, while Fig. 3d indicates a K_d of 5.7 ± 0.6 μM for nitroprofilin. The results thus indicate that profilin tyrosine nitration does not alter its affinity towards PIP_2.

Binding of Profilin/Nitroprofilin to PLP—A plot of change in the fluorescence (ΔF) *vs.* PLP concentration indicated more ΔF for nitroprofilin at lower concentrations upto 25 μM of PLP, whereas for profilin at concentrations above 25 μM of PLP (Fig. 4a). The relative affinities of profilin and nitroprofilin to PLP were determined through binding isotherms by plotting $\Delta F/\Delta F_{max}$ against PLP concentration. The binding isotherms (Fig. 4b) revealed that at different concentrations of PLP the amount of PLP bound is more for nitroprofilin than profilin, thus indicating higher affinity of nitroprofilin towards PLP than that of profilin. Further, the binding constant (K_d) was calculated from Scatchard plots, where $\Delta F/\Delta F_{max}$ was plotted against $\Delta F/\Delta F_{max}$/Lfree. Figure 4c indicates a K_d of 21 ± 1.7 μM for profilin, while Fig. 4d indicates a K_d of 1.1 ± 0.1 μM for nitroprofilin. Overall, the data point to a 20-fold increase in the affinity of nitroprofilin to PLP when compared to that of profilin.

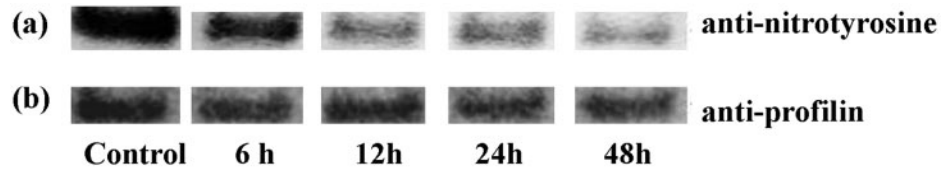

Fig. 2. **Carboxypeptidase Y digestion of nitroprofilin to map nitration sites.** Profilin in 100 mM potassium phosphate buffer, pH 7.4, was treated for 30 min with a 100-fold molar excess of peroxynitrite at room temperature. Nitroprofilin (150 μg), dialyzed against 100 mM citrate buffer, pH 6.0, was digested at room temperature with carboxypeptidase Y (10 μg, 1,000 mU) for 6, 12, 24 or 48 h. The addition of 5 mM PMSF stopped the reaction; proteins were separated by 10% SDS-PAGE, transferred to a nitrocellulose membrane, and then probed individually with (a) anti-nitrotyrosine and (b) anti-profilin antibodies. The blot is representative of two independent experiments.

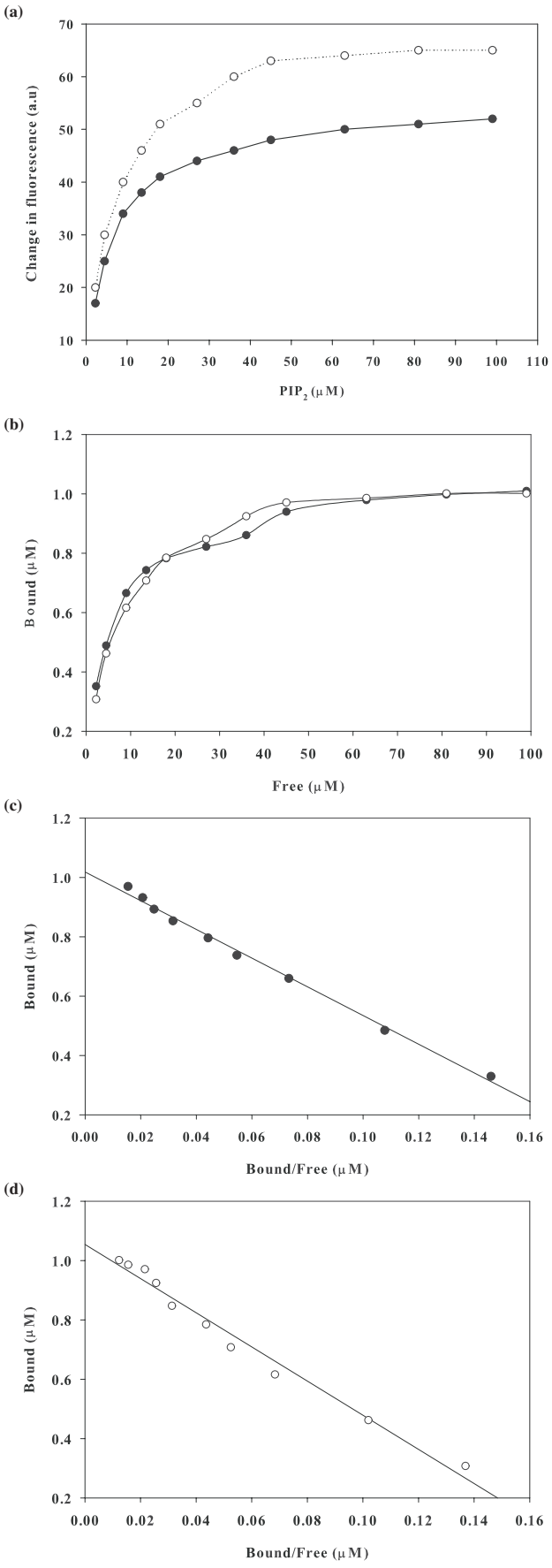

Effect of Nitroprofilin on Actin Polymerization—Actin polymerization decreased by 14.3% in the presence of profilin, while in the presence of nitroprofilin no significant change in polymerization was noted (Fig. 5). The critical actin monomer concentration under these conditions was found to be 110 nM with actin alone, which increased to 150 nM and 250 nM with nitroprofilin and profilin, respectively (Fig. 6), indicating nitroprofilin is not a better actin sequesterer.

DISCUSSION

Profilin has 4 tyrosines at positions 6 (helix 1, N-terminal), 26 (β-strand), 128 (helix 4), and 139 (turn, C-terminal). The C-terminus of profilin is of special interest because it contains a solvent-exposed tyrosine, Tyr 139, which is critical for its ligand interactions. Further, multiple sequence alignment of the carboxy terminal ends of profilins I from various animal sources using the ClustalW program (www.ebi.ac.uk/clustalW) indicated that tyrosine 139 is highly conserved in animals (Fig. 7).

Tyrosine nitration is a selective process and not all tyrosines in a protein undergo nitration. There are certain factors that determine the selectivity on nitration of tyrosine residues in proteins (*32*, *33*). Apparent structural requirements for the selectivity of protein tyrosine nitration are: (i) Paucity of reactive cysteine/methionine residues in the vicinity of tyrosine residues; (ii) proximity to a negatively charged residue; (iii) absence of steric hindrances; (iv) surface exposure (accessibility); and (v) preference for tyrosine residues in loop structures (*32*, *33*). The primary sequence of bovine profilin I (PDB ID: 1PNE) used for prediction analysis is given in Fig. 8. The above-mentioned criteria were checked as follows. The presence of Cys/Met and charged amino acids in the neighborhood of tyrosines was examined using SWISS-PDBVIEWER. Secondary structures and electrostatics were calculated using JOY and MOE, respectively. The solvent accessible surface areas were calculated using the g_sas module of the GROMACS software. Prediction based on the factors determining the selectivity for tyrosine nitration indicated tyrosine 139 to be the most potential site, as it satisfies the 1st,

Fig. 3. **Interaction of profilin and nitroprofilin with PIP_2.** (a) The change in tryptophan fluorescence emission (ΔF, in arbitrary units) for profilin (solid circles) and nitroprofilin (open circles) was plotted against different concentrations of PIP_2. The excitation wavelength (λ) was set at 295 nm. (b) Binding isotherm for profilin and nitroprofilin. The numbers of mol of PIP_2 bound per mol of profilin (solid circles) and nitroprofilin (open circles) were plotted against the concentration of free PIP_2. The ΔF_{max} values for profilin and nitroprofilin were obtained using linear regression. $\Delta F/\Delta F_{max}$ represents the number of mol of PIP_2 bound while the free PIP_2 concentration is assumed to be the amount of PIP_2 added. (c) Scatchard plot analysis of profilin binding to PIP_2. $\Delta F/\Delta F_{max}$ values were plotted against $(\Delta F/\Delta F_{max})$/LFree. $\Delta F/\Delta F_{max}$ represents the number of mol of PIP_2 bound and $(\Delta F/\Delta F_{max})$/LFree represents the bound/free PIP_2. The free ligand concentration is assumed to be the amount of PIP_2 added. (d) Scatchard plot analysis of nitroprofilin binding to PIP_2. The $\Delta F/\Delta F_{max}$ values of nitroprofilin were plotted against $(\Delta F/\Delta F_{max})$/LFree. $\Delta F/\Delta F_{max}$ represents the number of mol of PIP_2 bound and $(\Delta F/\Delta F_{max})$/LFree represents the bound/free PIP_2. The free ligand concentration is assumed to be the amount of PIP_2 added. K_d values represent the means ± SD of 4 independent experiments.

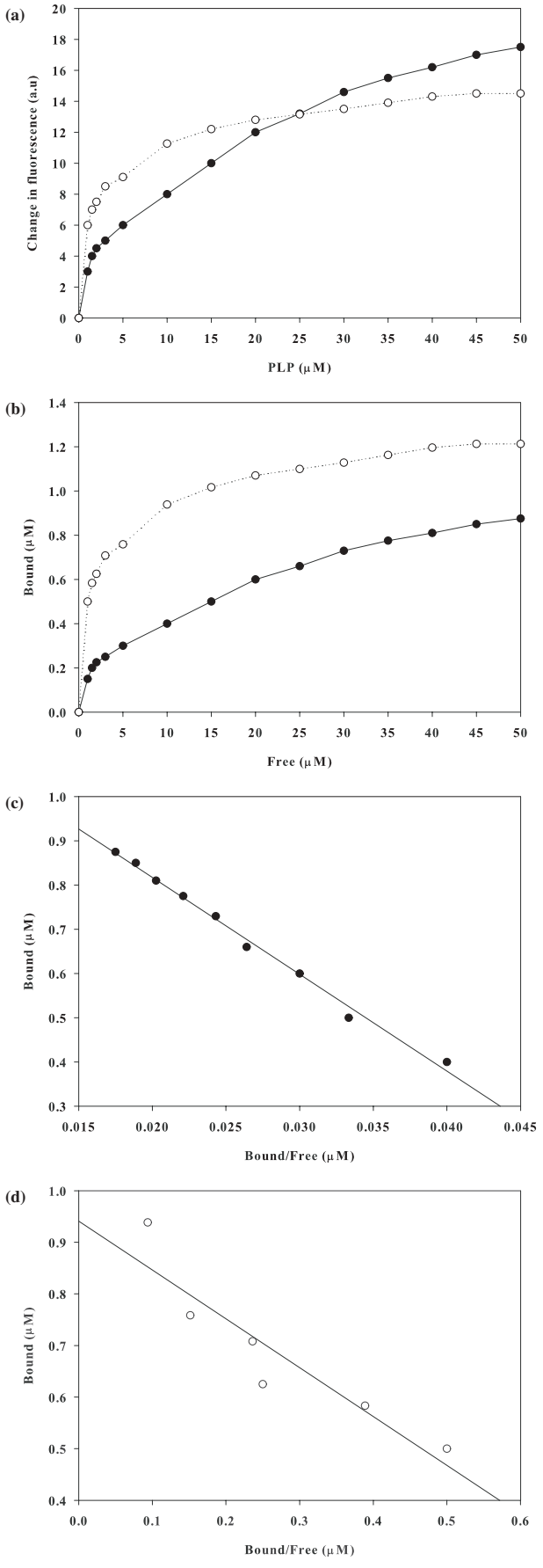

3rd, 4th and 5th criteria. Tyr139 has positively charged Lys and Arg residues in its vicinity, but its position is much more flexible, it being located in the loop structure, and having the maximum surface exposure for CE1 and CE2 atoms, and the absence of any steric hindrance, which favor its nitration. Though the presence of negatively charged Asp and Glu residues is favourable for Tyr 6, Tyr 24 and Tyr 128 to undergo nitration, they also have an unfavourable Met residue in their vicinity (column 2 in Table 1). Tyr128 has a negatively charged Glu residue, but undergoes steric restriction by surrounding side chains. Tyr139 has positively charged Lys and Arg residues in its vicinity, but its position is much more flexible, it being located in the loop structure, and having the maximum surface exposure for CE1 and CE2 atoms (CE1 and CE2 are the two equivalent carbons at the 3 and 5 positions of the aromatic ring, column 4 in Table 1). The CE2 atoms of Tyr 6, Tyr 24 and Tyr128 are surface accessible, while the CE1 atoms are buried compared to in the case of Tyr139 (column 4 in Table 1). Moreover, Tyr6, Tyr24 and Tyr128 comprise part of secondary structures, while Tyr 139, being in a loop structure, exhibits more conformational freedom for its interaction with a nitrating agent (column 3 in Table 1). Thus, the presence of Tyr 139 in the loop region, the absence of any steric hindrance, and the high surface accessibility of CE1 and CE2 atoms favors the nitration of Tyr 139.

Immunoblots probed with anti-nitrotyrosine antibodies showed a peroxynitrite concentration-dependent increase in the nitrotyrosine level. As nitrotyrosine shows specific absorbance at 428 nm, we quantitated nitrotyrosine residues in profilin upon peroxynitrite treatment. The data presented indicate a correlation between the amounts of nitrotyrosine detected with antibodies and determined by spectrophotometric analysis. The stoichiometry of 0.6 (moles of nitrotyrosine/mole of profilin) indicated that a single tyrosine residue is nitrated in profilin. As a step towards identifying nitrotyrosine residues in profilin, digestion of nitroprofilin with carboxypeptidase Y was performed. Carboxypeptidase digestion of profilin releases carboxy-terminal Y easily, and S and Q slowly (*37*). The decrease in nitrotyrosine-immunoreactivity of nitroprofilin

Fig. 4. **Interaction of profilin and nitroprofilin with PLP.** (a) The change in tryptophan fluorescence emission (ΔF, in arbitrary units) for profilin (solid circles) and nitroprofilin (open circles) was plotted against different concentrations of poly (L-proline). The excitation wavelength (λ) was set at 295 nm. (b) Binding isotherm for profilin and nitroprofilin. The numbers of mol of poly (L-proline) bound per mol of profilin (solid circles) and nitroprofilin (open circles) were plotted against the concentration of free PLP. The ΔF_{max} values for profilin and nitroprofilin were obtained from double reciprocal plots of $1/\Delta F$ *vs.* 1/poly (L-proline) using linear regression. $\Delta F/\Delta F_{max}$ represents the number of mol of PLP bound, while the free ligand concentration is assumed to be the amount of PLP added. (c) Scatchard plot analysis of profilin binding to PLP. $\Delta F/\Delta F_{max}$ values of profilin were plotted against $(\Delta F/\Delta F_{max})$/LFree. $\Delta F/\Delta F_{max}$ represents the number of mol of PLP bound and $(\Delta F/\Delta F_{max})$/LFree represents the bound/free PLP. Free PLP concentration is assumed to be the amount of PLP added. (d) Scatchard plot analysis of nitroprofilin binding to PLP. The $\Delta F/\Delta F_{max}$ values of profilin were plotted against $(\Delta F/\Delta F_{max})$/LFree. The $\Delta F/\Delta F_{max}$ represents the number of mol of PLP bound and $(\Delta F/\Delta F_{max})$/LFree represents the bound/free PLP. The free PLP concentration is assumed to be the amount of PLP added. Kd values represent the means ± SD of 4 independent experiments.

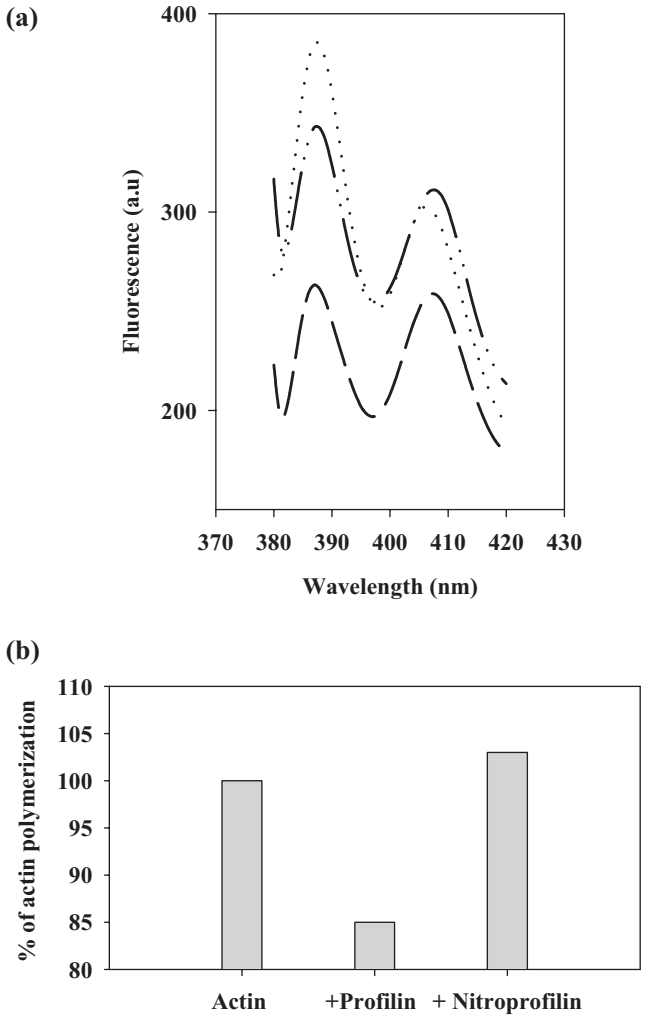

Fig. 5. **Effects of profilin and nitroprofilin on actin polymerization.** 2 μM G-actin (10% pyrene-labeled) was pre-incubated with 2 μM profilin or nitroprofilin for 15 min. Actin polymerization was measured by suspending the mixture in F-buffer and then measuring the increase in fluorescence (excitation at 365 nm and emission from 380 to 420 nm) at different times. (a) The emission spectra presented are (i) G-actin in F-buffer at 30 min (. . .), (ii) G-actin with profilin in a 1:1 ratio in F-buffer at 30 min (– –), and (iii) G-actin with nitroprofilin in a 1:1 ratio in F-buffer after 30 min (–. . .–) (b) Percentage of actin polymerization in the presence of profilin and nitroprofilin, with emission at 407 nm. Lane 1, actin alone; lane 2, actin in the presence of profilin; and lane 3, actin in the presence of nitroprofilin.

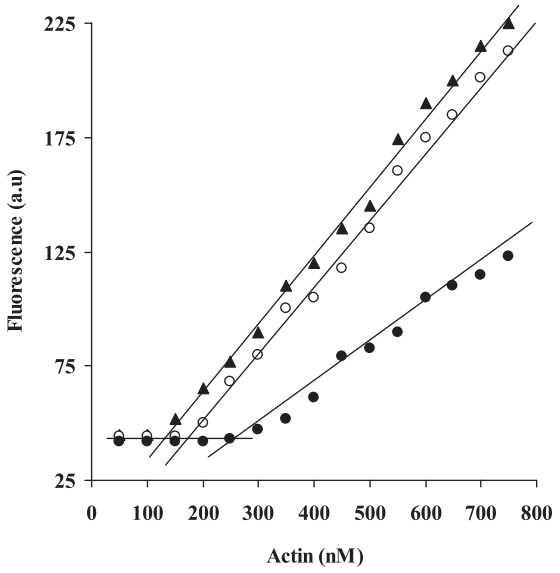

Fig. 6. **Effects of profilin and nitroprofilin on the actin critical monomer concentration.** G-actin (2 μM, 10% pyrene-labeled), and profilin and nitroprofilin (2 μM each) were pre-incubated in F-buffer for 16 h. The decrease in fluorescence in serially diluted samples was noted. The excitation and emission wavelengths were set at 365 nm and 407 nm, respectively. (Δ) Actin alone, (open circles) actin in the presence of profilin, and (solid circles) actin in the presence of nitroprofilin.

```
FABO          TAKTLVLLMGKEGVHGGMINKKCYEMASHLRRSQY 139
1PNE          TAKTLVLLMGKEGVHGGMINKKCYEMASHLRRSQY 140
P02584        TAKTLVLLMGKEGVHGGMINKKCYEMASHLRRSQY 139
AAX09095.1    TAKTLVLLMGKEGVHGGMINKKCYEMASHLRRSQY 140
S04067        TAKTLVLLMGKEGVHGGLINKKCYEMASHLRRSQY 140
P62962        TAKTLVLLMGKEGVHGGLINKKCYEMASHLRRSQY 140
P62963        TAKTLVLLMGKEGVHGGLINKKCYEMASHLRRSQY 140
AAH13439.1    TDKTLVLLMGKEGVHGGLINKKCYEMASHLRRSQY 140
1CF0          TDKTLVLLMGKEGVHGGLINKKCYEMASHLRRSQY 138
NP_005013.1   TDKTLVLLMGKEGVHGGLINKKCYEMASHLRRSQY 140
P07737        TDKTLVLLMGKEGVHGGLINKKCYEMASHLRRSQY 140
AAH02475.1    TDKTLVLLMGKEGVHGGLINKKCYEMASHLRRSQY 140
AAH06768.1    TDKTLVLLMGKEGVHGGLINKKCYEMASHLRRSQY 140
AAH15164.1    TDKTLVLLMGKEGVHGGLINKKCYEMASHLRRSQY 140
AAH57828.1    TDKTLVLLMGKEGVHGGLINKKCYEMASHLRRSQY 140
```

Fig. 7. **Multiple sequence alignment of the profilin carboxy terminal sequence.** The profilin I sequences of different animal sources were aligned using ClustalW (www.ebi.ac.uk/clustalW).

upon carboxypeptidase digestion and the stoichiometry of 0.6 (moles of nitrotyrosine/mole of profilin) indicate a single tyrosine residue at the C-terminal end (Tyr 139) was nitrated.

Tyrosine nitration alters protein function by inducing substantial structural changes and tyrosine reactivity. It decreases the pK_a of tyrosine from 10 to about 7, introduces a negative charge that can alter the local structure of proteins, and the hydrogen bonding activities of tyrosine with substrates and neighbouring amino acids, and the bulky nitro group induces steric perturbation in the structure of tyrosine, which may inhibit the binding of substrates to enzymes or disrupt protein–protein interactions in which tyrosine residues are instrumental (*38*). Thus, the present data on nitration of Tyr 139 of profilin create a basis for further studies on the effects of tyrosine nitration on structure and the interaction with three of its ligands *vis a vis* poly (L-proline), phosphoinositides and actin.

Table 1. **Surface exposure, secondary structure and amino acids in vicinity of tyrosine residues in profilin.** @CE1 and CE2 are the two equivalent carbons at the 3 and 5 positions of the aromatic ring. Solvent-accessible surfaces were calculated using the g_sas module in the GROMACS software. The total solvent-accessible surface of the proteins was determined by rolling a 1.4 Å-radius probe over the vander Waals surface of the entire structure. The crystal structure file 1PNE.pdb for profilin was used for the analysis. The residues within 5 Å of tyrosine residues were found using the SwissPDBviewer software.

Res. No.	Residues in vicinity of 5 Å	2° Structure	Surface exposure		
			OH (Å^2)	CE1 (Å^2)@	CE2 (Å^2)@
Tyr 6	GWNAIDLMHL	Helix	23.57	9.90	13.21
Tyr 24	VPDKELMTA	Sheet	36.32	0.00	13.21
Tyr 128	SAMEKCINTG	Helix	23.57	13.21	16.51
Tyr 139	WTKAQRS	Loop	25.92	23.11	16.51

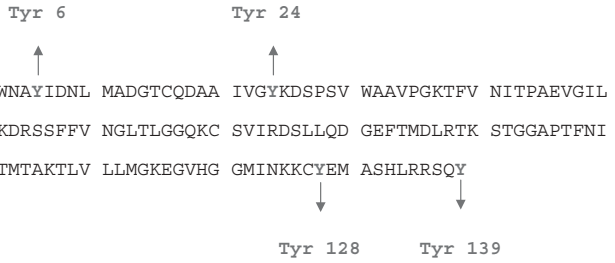

Fig. 8. **Primary sequence of bovine profilin I.** Primary sequence of bovine profilin I (PDB ID, 1PNE) obtained from a protein data bank (http://www.rcsb.org). Tyrosine residues are numbered with arrows.

Fluorescence (*39*), mutagenesis (*40*, *41*), and qualitative NMR (*39*, *42*) studies indicated a highly conserved patch of six hydrophobic amino acids (W3, Y6, W31, H133, L134 and Y139) to be the PLP binding site. In the present study we monitored the interaction of profilin and nitroprofilin with PLP, by exploiting the quenching of tryptophan fluorescence. Binding isotherm and Scatchard plot analysis revealed that nitroprofilin exhibits high affinity towards PLP sequences.

Our earlier data on C-terminal serine phosphorylated profilin indicated no change in affinity towards PIP_2, thus strongly suggesting the charge at C-terminal end plays no role in phosphatidylinositol binding (*34*). In the present study fluorescence quenching of Trp3 and Trp31 has been exploited for studying the interaction of profilin and nitroprofilin with PIP_2. On introducing a net negative charge by nitration of the C-terminal Tyr 139 of profilin, we did not observe any significant difference in relative fluorescence ($\Delta F/\Delta F_{max}$) for either profilin or nitroprofilin. Further, binding isotherm and Scatchard plot analysis revealed no change in the affinity of profilin towards PIP_2 upon nitration. Since nitration has no influence on PIP_2 binding, our data strongly suggest that a charge at the C-terminal end may not be important for phosphatidylinositol binding. Since nitroprofilin exhibits similar affinity to PIP_2 to that of profilin, profilin nitration might not influence its association with PIP_2 and thus not its localization to membranes.

Nitration of many actin-binding proteins leads to either maintenance or alteration of actin-binding functions. This was supported by loss of filament growth control by actin; altered cytoskeletal morphology, intracellular localization of the cytoplasmic motor protein dynein, and changes in microtubule structure and organization caused by α-tubulin upon nitration (*43*, *44*). The effect of nitroprofilin on actin polymerization was studied by using *N*-(1-pyrenyl) iodoacetamide–labeled actin, and by calculating the *in vitro* critical actin monomer concentrations in the presence of profilin and nitroprofilin. The actin critical monomer concentration data indicate that nitroprofilin is not a better actin sequesterer.

In a number of pathological conditions (inflammatory conditions) peroxynitrite formation and protein nitration are well documented, but little is known about the direct involvement of a particular protein in these diseases. Drugs that inhibit protein nitration are very promising for inhibiting platelet aggregation. Many proline-rich proteins like VASP, Ena and Mena (*45*, *46*) involved in the regulation of actin polymerization are known to recruit profilin to membranes, thus driving cell motility and other actin-linked processes (*47*). The data presented here indicate that profilin-protein interactions could be regulated by nitration. The increased affinity of nitroprofilin to PLP indicates an important mechanism whereby profilin could specifically bind selective proteins and then recruit them to the sites of rapid actin polymerization or plasma membranes, where it can selectively bind PIP_2 and PLP. However, the significance of profilin nitration in pathophysiological conditions needs to be evaluated.

REFERENCES

1. Radi, R., Peluo, G., Alvarez, M.N., Naviliat, M., and Cayota. A. (2001) Uraveling peroxynitrite formation in biological systems. *Free Radic. Biol. Med.* **30**, 463–488
2. Rodenas, J., Carbonell, T., and Metjavila, M.T. (2000) Different roles for nitrogen monoxide and peroxynitrite in lipid peroxidation induced by activated neutrophils. *Free Radic. Biol. Med.* **28**, 374–380
3. Burney, S., Cauleld, J.L., Niles, J.C., Wishnok, J.S., and Tannenbaum, S.R. (1999) The chemistry of DNA damage from nitric oxide and peroxynitrite. *Mutat. Res*. **424**, 37–49
4. Radi, R. (2004) Nitric oxide, oxidants, and protein tyrosine nitration. *Proc. Natl. Acad. Sci. USA* **101**, 4003–4008
5. Arteel, G.E., Briviba, K., and Sies, H. (1999) Protection against peroxynitrite. *FEBS Lett.* **445**, 226–230
6. Berlett, B.S., Friguet, B., Yim, M.B., Chock, P.B., and Stadtman, E.R. (1996) Peroxynitrite-mediated nitration of tyrosine residues in *Escherichia coli* glutamine synthetase mimics adenylylation: relevance to signal transduction. *Proc. Natl. Acad. Sci. USA* **93**, 1776–1780
7. Zou, M., Martin, C., and Ullrich, V. (1997) Tyrosine nitration as a mechanism of selective inactivation of prostacyclin synthase by peroxynitrite. *Biol. Chem.* **378**, 707–713
8. Roberts, E.S., Lin, H.L., Crowley, J.R., Vuletich, J.L., Osawa, Y., and Hollenberg, P.F. (1998) Peroxynitrite-mediated nitration of tyrosine and inactivation of the

catalytic activity of cytochrome P450. *Chem. Res. Toxicol.* **11**, 1067–1074
9. Daiber, A., Herold, S., Schoeneich, C., Namgaladze, D., Peterson, J.A., and Ullrich, V. (2000) Nitration and inactivation of cytochrome P450 BM-3 by peroxynitrite. Stopped flow measurements prove ferryl intermediates. *Eur. J. Biochem.* **267**, 6729–6739
10. Blanchard-Fillion, B., Souza, J.M., Friel, T., Jiang, G.C.T., Vrana, K., Sharov, V., Barron, L., Schoneich, C., Quijano, C., Alvare, B., Radi, R., Przedborski, S., G.S. Fernando, G.S., Horwitz, J., and Ischiropoulos. H. (2002) Nitration and inactivation of tyrosine hydroxylase by peroxynitrite. *Biol. Chem.* **276**, 46017–46023
11. Viner, R.I., Ferrington, D.A., Williams, T.D., Bigelow, D.J., and Schoneich, C. (1999) Protein modification during biological aging: selective tyrosine nitration of the SERCA2a isoform of the sarcoplasmic reticulum Ca^{2+}-ATPase in skeletal muscle. *Biochem. J.* **340**, 657–669
12. Szabo, C. (2003) Multiple pathways of peroxynitrite cytotoxicity. *Toxicol. Lett.* **141**, 105–112
13. Romeo, G., Frangioni, J.V., and Kazlauskas, A. (2004) Profilin acts downstream of LDL to mediate diabetic endothelial cell dysfunction. *FASEB J.* **18**, 725–727
14. Beckman, J.S. and Koppenol, W.H. (1996) Nitric oxide, superoxide, and peroxynitrite: the good, the bad, and ugly. *Am. J. Physiol.* **271**, C1424–C1437
15. Beckman, J.S. (1994) Oxidative damage and tyrosine nitration from peroxynitrite. *Chem. Res. Toxicol.* **9**, 836–844
16. Sabetkar, M., Low, S.Y., Naseem, K.M., and Bruckdorfer, K.R. (2002) The nitration of proteins in platelets: significance in platelet function. *Free Radic. Biol. Med.* **33**, 728–736
17. Lassing, I. and Lindberg, U. (1988) Specificity of the interaction between PIP_2 and the profilin: actin complex. *J. Cell Biochem.* **37**, 255–267
18. Lu, J. and Pollard, T.D. (2001) Profilin binding to poly-L-proline and actin monomers along with ability to catalyse actin nucleotide exchange is required for viability of fission yeast. *Mol. Biol. Cell.* **12**, 1161–1175
19. Vojtek, A., Haarer, B., Field., Gerst, J., Pollard, T.D., Brown, S., and Wigler, M. (1991) Evidence for a functional link between profilin and CAP in the yeast *S. cerevisiae. Cell* **66**, 497–505
20. Domann, E., Wehland, J., Rhode, M., Pistor, S., Hartl, M., Goebel, W., Lemeister-Wachter, M., Wuenscher, M., and Chakraborthy, T.C. (1992) A novel bacteria virulence gene in *Listeria monocytogenes* required for host cell microfilament interaction with homology to the proline-rich region in vinculin. *EMBO J.* **11**, 1981–1990
21. Metzler, W.J., Ernst, E., Lavoie, T.B., and Mueller, L. (1994). Identification of poly L-proline binding site on human profilin. *J. Biol. Chem.* **269**, 4620–4625
22. Kaiser, D.A. and Pollard, T.D. (1996) Characterization of actin and poly-L-proline binding sites of *Acanthamoeba* profilin with monoclonal antibodies and by mutagenesis. *J. Mol. Biol.* **255**, 89–107
23. Bjorkegren, C., Rozycki, M.D., Schutt, C.E., Lindberg, U., and Karlsson, R. (1993) Mutagenesis of human profilin locates its poly (L-proline)-binding site to a hydrophobic patch of aromatic amino acids. *FEBS Lett.* **333**, 123–126
24. Archer, S.J., Vinson, V.K., Pollard, T.D., and Torchia, D.A. (1994) Elucidation of poly L-proline site in *Acanthamoeba* profilin I by NMR spectroscopy. *FEBS Lett.* **337**, 145–151
25. Sohn, R.H., Chen, J., Koblan, K.S., Bray, P.F., and Goldschmidt-Clermont, P.J. (1995) Localization of a binding site for phosphatidylinositol 4,5-bisphosphate on human profilin. *J. Biol. Chem.* **270**, 21114–21120
26. Yu, F.X., Sun, H.Q., Janmey, P.A., and Yin, H.L. (1992) Identification of a polyphosphoinositide-binding sequence in an actin monomer-binding domain of gelsolin. *J. Biol. Chem.* **267**, 14616–14621
27. Bhargavi, V. and Singh, S.S. (2001) Protein kinase C isozyme-specific phosphorylation of profilin. *Cellular Signalling* **13**, 433–439
28. Lowry, O.H., Roebrough, N.J., Farr, A.L., and Randall, R.J. (1951) Protein measurement with the Folin-phenol reagent. *J. Biol. Chem.* **193**, 265–275
29. Schagger, H. and von Jagow, G. (1987) Tricine-sodium dodecyl sulphate polyacrylamide gel electrophoresis for the separation of proteins in the 1 to 100 kD range. *Anal. Biochem.* **166**, 368–379
30. Beckman, J.S., Beckman, T.W., Chen, J., Marshall, P.A., and Freeman, B.A. (1990) Apparent hydroxyl radical production by peroxynitrite: implications for endothelial injury from nitric oxide and superoxide. *Proc. Natl. Acad. Sci. USA* **87**, 1620–1624
31. Hughes, M.N. and Nicklin, H.G. (1968) *J. Am. Chem. Soc.* 450–452
32. Ischiropoulos, H. (2003) Biological selectivity and functional aspects of protein tyrosine nitration. *Biochem. Biophys. Res. Commun.* **305**, 776–83
33. Souza, J.M., Daikhin, E., Yudkoff, M., Raman, C.S., and Ischiropoulos, H. (1999) Factors determining the selectivity of protein tyrosine nitration. *Arch. Biochem. Biophys.* **371**, 169–178
34. Sathish, K., Padma, B., Munugalavadla, V., Bhargavi, V. Radhika, K.V.N., Wasia, R., Sairam, M., and Surya, S.S. (2004) Phosphorylation of profilin regulates its interaction with actin and poly (L-proline). *Cellular Signalling* **16**, 589–596
35. Kouyama, P. and Mihashi, K. (1981). Fluorimetry study of N-(1-pyrenyl) iodoacetamide-labelled F-actin. *Eur. J. Biochem.* **114**, 33–38
36. Bhargavi, V., Chari, V.B., and Singh, S.S. (1998) Phosphatidylinositol 3-kinase binds to profilin through the p85α subunit and regulates cytoskeletal assembly. *Biochem. Mol. Biol. Int.* **46**, 241–248
37. Malm, B., Larsson, H., and Lindberg, U. (1983) The profilin-actin complex: further characterization of profilin and studies on the stability of the complex. *J. Muscle Res. Cell Motil.* **4**, 569–568
38. Eiserich, J.P., Estevez, A.G., Bamberg, T.V., Ye, Y.Z., Chumley, P.H., Beckman, J.S., and Freeman, B.A. (1999) Microtubule dysfunction by posttranslational nitrotyrosination of alpha-tubulin: a nitric oxide-dependent mechanism of cellular injury. *Proc. Natl. Acad. Sci. USA* **96**, 6365–6370
39. Metzler, W.J., Ernst, E., Lavoie, T.B., and Mueller, L. (1994). Identification of poly L-proline binding site on human profilin. *J. Biol. Chem.* **269**, 4620–4625
40. Kaiser, D.A. and Pollard, T.D. (1996) Characterization of actin and poly-L-proline binding sites of *Acanthamoeba* profilin with monoclonal antibodies and by mutagenesis. *J. Mol. Biol.* **255**, 89–107
41. Bjorkegren, C., Rozycki, M.D., Schutt, C.E., Lindberg, U., and Karlsson, R. (1993) Mutagenesis of human profilin locates its poly (L-proline)-binding site to a hydrophobic patch of aromatic amino acids. *FEBS Lett.* **333**, 123–126
42. Archer, S.J., Vinson, V.K., Pollard, T.D., and Torchia, D.A. (1994) Elucidation of poly L-proline site in *Acanthamoeba* profilin I by NMR spectroscopy. *FEBS Lett.* **337**, 145–151
43. Chang, Daniel, R.W., Ambar, Salam, Dorota, G., Aparna Prasad, Eiserich, J.P., and J. Bulinski, J.C. (2002) Alteration of the C-terminal amino acid of tubulin specifically inhibits myogenic differentiation. *J. Biol. Chem.* **277**, 30690–30698
44. Aslan, M., Ryan, T.M., Townes, T.M., Coward, L., Kirk, M.C., Barnes, S., Alexander, C.B., Rosenfeld, S.S., and Freeman, B.A. (2003) Nitric oxide-dependent generation of reactive species in sickle cell disease. Actin tyrosine induces defective cytoskeletal polymerization. *J. Biol. Chem.* **278**, 4194–4204
45. Reinhard, M., Giehl, K., Abel, K., Haffner, C., Jarchau, T., Hoppe, V., Jockusch, B.M., and Walter, U. (1995) The

proline-rich focal adhesion and microfilament protein VASP is a ligand for profilins. *EMBO J.* **14**, 1583–1589

46. Gertler, F.B., Niebuhr, K., Reinhard, M., Wehland, J., and Soriano, P. (1996) Mena, a relative of VASP and *Drosophila* enabled, is implicated in the control of microfilament dynamics. *Cell* **87**, 227–239

47. Chakraborthy, T., Ebel, F., Domann, E., Niebuhr, K., Gerstel, B., Pistor, S., Temm-Grove, C.J., Jockusch, B.M., and Reinhard, M., Walter, U., and Wehland, J. (1995) A focal adhesion factor directly linking intracellularly motile *Listeria* monocytogenes and *Listeria ivanovii* to the actin-based cytoskeleton of mammalian cells. *EMBO J.* **14**, 1314–1321